A first CO(J = 2 - 1) survey of the southern Milky Way

Israel, F.P.; Graauw, Th. de; Biezen, J. van der; Vries, C.P. de; Brand, J.; Habing, H.J.; ... ; Selman, F.

Astron. Astrophys. 134, 396–401 (1984)

ASTRONOMY AND ASTROPHYSICS

A first CO($J=2-1$) survey of the southern Milky Way*

F. P. Israel[1], Th. de Graauw[1], C. P. de Vries[2], J. Brand[2], H. van de Stadt[3], H. J. Habing[2], J. G. A. Wouterloot[4], J. van Amerongen[3], J. van der Biezen[1], A. Leene[2], I. Nagtegaal[3], and F. Selman[5]

[1] ESTEC, European Space Agency, Postbus 299, 2200 AG Noordwijk, The Netherlands
[2] Sterrewacht, Huygens Laboratory, Leiden, The Netherlands
[3] Sterrewacht Sonnenborgh, Utrecht, The Netherlands
[4] ESO, Karl-Schwarzschild-Strasse 2, D-8046 Garching bei München, Federal Republic of Germany
[5] Universidad de Chile, Santiago, Chile

Received September 2, accepted November 16, 1983

Summary. The fourth galactic quadrant ($l=270°$–$355°$) was surveyed in the CO($J=2-1$) transition at a wavelength of 1.3 mm. The CO(2–1) distribution strongly resembles the CO(1–0) distribution in the same quadrant; it is found to be clumpy and contains a number of "holes". The radial distribution of CO in the fourth quadrant differs from that in the (northern) first quadrant and shows a broader maximum with peaks at $R=4$ and $R=8$ kpc. The cloud-cloud velocity dispersion is, however, very similar to that found in the northern hemisphere; it is of order 4 km s^{-1}.

Key words: galactic structure – surveys – southern Milky Way – CO(2–1) observations

1. Introduction

Observations carried out over the last decade have shown that the CO molecule is an excellent tracer of molecular clouds in the galaxy. However, because of the uneven distribution of observatories over the world, favouring the northern hemisphere, the distribution and properties of molecular material in the southern Galaxy are poorly explored subjects. For this reason, we have carried out a first survey of southern molecular clouds in the CO($J=2-1$) transition, using the telescopes of the European Southern Observatory at La Silla (Chile). The survey consists of three parts: a survey of molecular clouds associated with H II regions, a survey of globules, dark clouds, reflection nebulae and Herbig-Haro type objects, and a survey of the galactic plane at $b=0°$ from $l=270°$ to $l=355°$. The results of the first two parts are described elsewhere (Brand et al., 1984; de Vries et al., 1984). In this paper we report on the results obtained in the galactic plane survey. It should be noted that this is the first galactic survey in the CO($J=2-1$) transition; the results are therefore complementary to southern hemisphere CO($J=1-0$) surveys such as the one carried out by the Australian group at Epping (Robinson et al., 1983) and the one currently in progress at CTIO (Cohen, 1983).

2. Observations and reduction

All observations described in this paper were made with the Estec-Utrecht submillimeter line receiver and the 1.4 m Coudé Auxiliary Telescope (CAT) at ESO La Silla in the period May 1981 to April 1982. This optical telescope was designed and built to feed the Coudé Echelle Spectrograph (CES) located at the coudé floor of the 3.6 m telescope building; it has a three-mirror coudé arrangement with an $f/120$ beam. We replaced one of the four secondary mirrors available in the mirror turret in order to obtain an $f/30$ beam suitable to feed the receiver frontend in the CAT dome. An additional polyethylene lens was used to match the $f/30$ optics to the receiver $f/9$ beam. The peculiar optical arrangement of the CAT with a rotating third mirror introduced considerable baseline ripple due to LO and mixer noise power reflected by the telescope and dome structure. With absorbing material at the center and edges of the secondary mirror, the amplitude of this ripple could be reduced; however, the greatest reduction came from using a wobbling mirror (Gustincic, 1976) which continuously varied the optical pathlength by half a wavelength during integration. This had the effect of making the noise power reflected into the mixer considerable less frequency dependent.

During the survey, the receiver system (Lidholm and de Graauw, 1979) used uncooled Schottky diode mixers with noise temperatures (DSB) around 1750 K. The NRAO type backend consisted of 256 channels of 1 MHz bandwidth and 256 channels of 250 kHz bandwidth. Consequently, the resolving powers at 230 GHz were 1.3 and 0.3 km s^{-1}, respectively, covering velocity ranges of 333 and 88 km s^{-1}. DSB calibration of the receiver was done by measuring hot and ambient temperature loads; beam profile and beam efficiency were determined by scanning the Moon. A beam size of 5′.5 (HPBW) was found. Overall system efficiency and atmospheric transmission were determined by measuring apparent sky temperatures at different airmasses; overall system efficiency on extended sources was 0.35, and during observations atmospheric transparency at the zenith was usually better than 85% (see also Brand, 1982; Sherwood et al., 1983; Brand, Sherwood, and van de Stadt, in preparation). In the following, we will use antenna temperatures T_A^* as defined by Kutner and Ulich (1981); Orion A then has an observed $T_A^*=36\pm1$ K, which is appropriate in view of source and telescope parameters.

We took all data in a position switching mode. Reference positions were generally taken several degrees away. We verified that these positions were free of CO line emission to a level several times below the general noise level of 0.5 K of the survey. We sampled essentially a grid with 30′ spacing, although sometimes a denser grid was used (up to a 7′.5 sampling). However, in order to obtain a sufficient signal-to-noise ratio we found it necessary to construct maps in which gridpoints were averaged over one degree

Send offprint requests to: F. P. Israel

* Based on observations made at the European Southern Observatory, La Silla, Chile

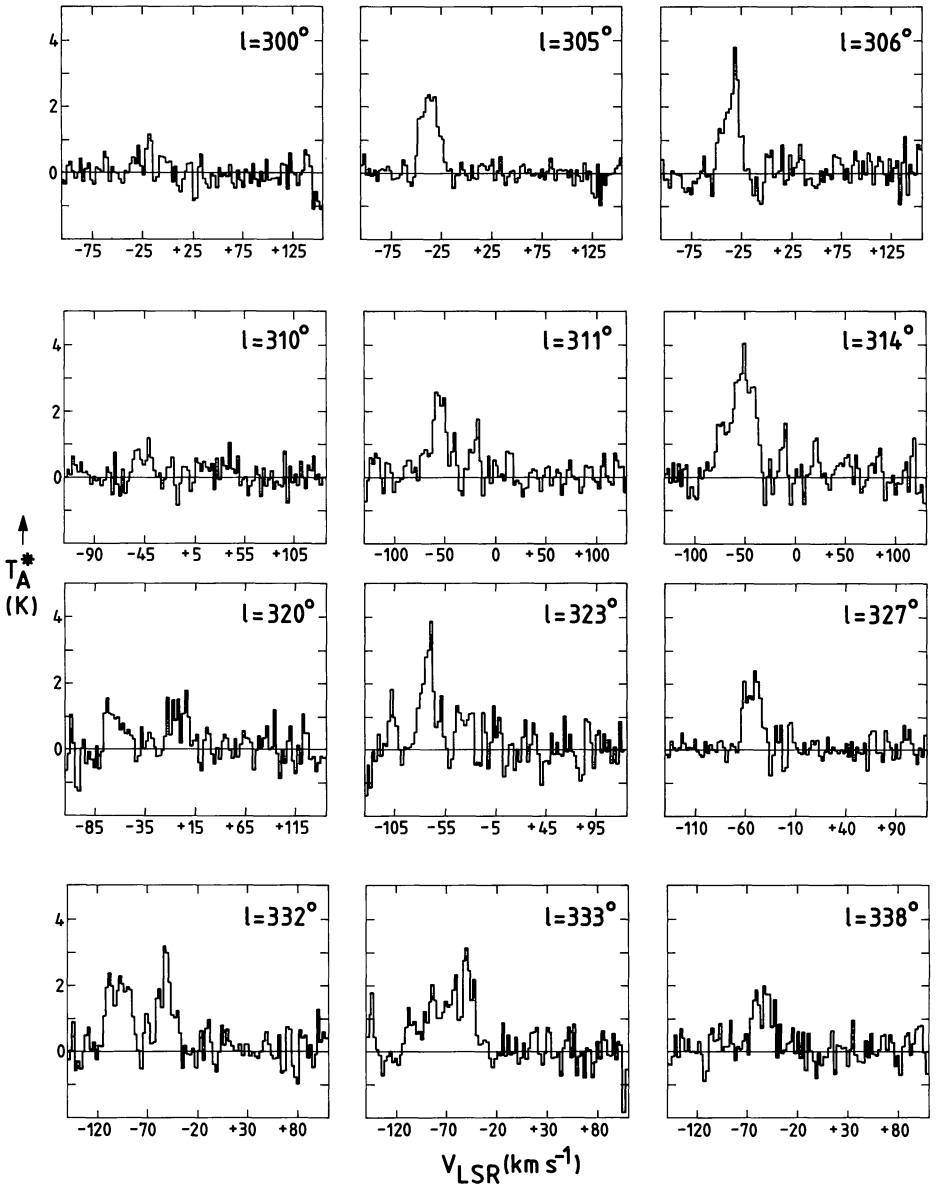

Fig. 1. Set of representative profiles obtained at various longitudes. Baselines have been corrected for both standing wave patterns and a slow variation (see text). Profiles are averages over one degree in longitude; individual channels are averaged two by two to a velocity resolution of 2.6 km s^{-1}

and two degree intervals. The resulting noise level is then 0.4 K in the $l=270°$–$330°$ interval and increases to 0.8 K from $l=330°$ to $l=355°$. This noise increase is largely due to shorter total integration times caused by the lesser visibility of longitudes near the Galactic Center because of the geometry of the CAT and 3.6 m telescope domes. As mentioned above, a major factor contributing to baseline uncertainties were reflections inside the telescope structure. Since the most important reflecting surfaces were located around the secondary mirror, the resulting baseline ripple shows up primarily as a sharply defined sinusoid with a single wavelength corresponding to the distance between the receiver and the secondary mirror. This being the case, it was easy to remove this sinusoid by means of filtering out the corresponding spatial frequency in the Fourier domain. This, of course, also alters the actually present CO signal, but the distortion of the CO emission profile was usually small with respect to the noise because the level of the power spectrum on both sides of the baseline-ripple frequency was usually close to the noise-level.

Very low frequency baseline variation were removed by eye estimate. Removal of this slow variation brings, however, with it the danger of also removing or decreasing weak and broad (typically 50 km s^{-1} or more) CO emission whenever present. Because of the kinematic properties of the Galaxy as viewed from the eccentric Solar position, this effect becomes increasingly significant at longitudes $l>320°$. Consequently, at these longitudes some fraction of low-level diffuse emission might have been removed, thereby enhancing the contrast of the remaining narrower structure which is still correctly represented. Obviously, determinations of CO emission integrated over velocity suffer most strongly from this effect.

In Fig. 1 we show a set of representative profiles at various galactic longitudes. These profiles represent averages over a degree in longitude and are averaged in velocity over 2 MHz (corresponding to a velocity resolution of 2.6 km s^{-1}).

3. Results

3.1. Velocity-longitude distribution

We have constructed a longitude-velocity map of the CO($J=2-1$) distribution of the fourth galactic quadrant (at

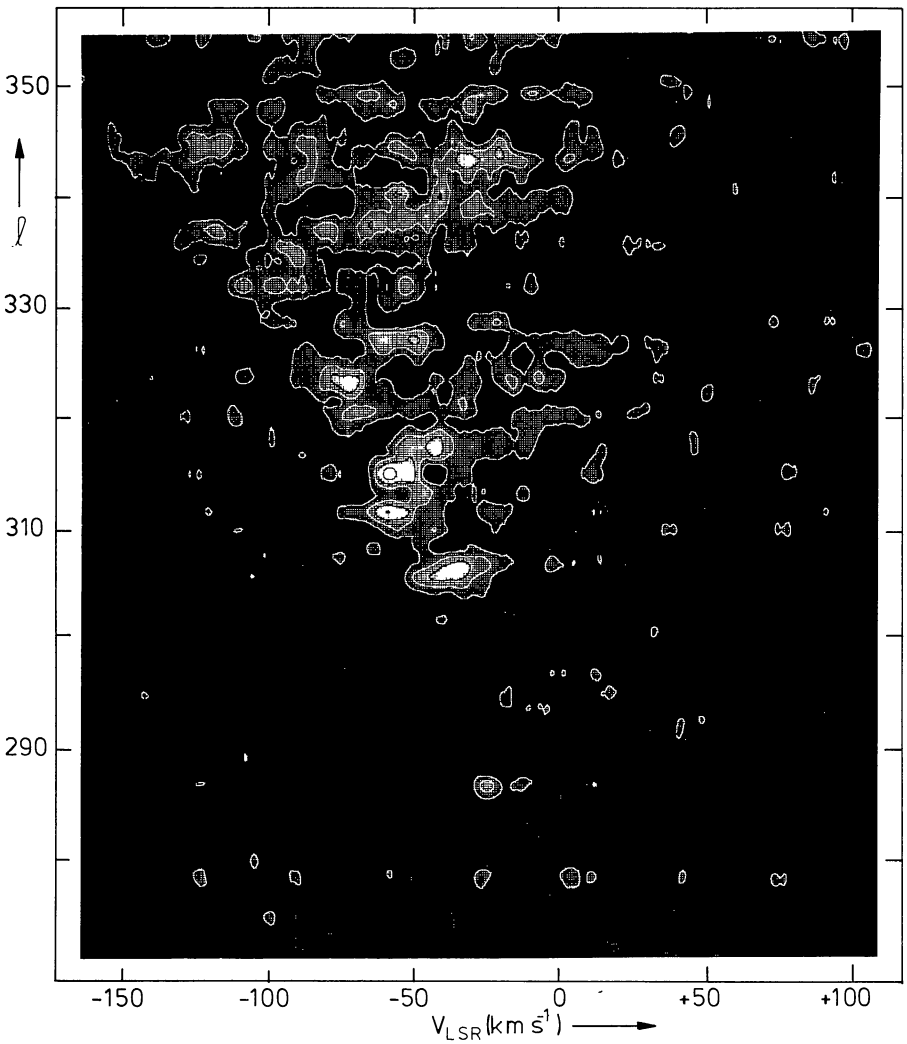

Fig. 2. Map of the CO($J=2-1$) distribution in the Galactic plane, between longitudes 270° and 355°. Contours are at intervals of 0.75 K, starting at 0.75 K. Sampling was at intervals of 30′, but the map has been smoothed to an effective resolution of two degrees and 5 km s^{-1}

$b=0°$) averaged over velocity intervals of 5 km s^{-1} and longitude intervals of 2° (Fig. 2) and also a map averaged over the same velocity interval, but over a longitude interval of one degree (Fig. 3). This must be compared with a beam resolution of 5′.5 and a sampling interval of 30′. The latter map covers only a limited range ($l=300°$–$335°$), but is based on generally higher-quality spectra, i.e. a noise level of 0.4 K maximum, as compared to a maximum noise level of 0.8 K as applicable to Fig. 2 (see preceding section). On the basis of mainly the latter map we have listed the intensities and sizes of the brightest CO($J=2-1$) maxima (Table 1); sizes given are extent in longitude deconvolved by the telescope beam; all clouds with peak $T_A^*>2.0$ K are listed. It is clear from Table 1 that the relatively large beam and the effect of averaging over large intervals conspire to dilute intensities considerably. Integrated intensities should, however, be affected to a lesser degree. We note that the general lack of CO shortwards of $l=300°$ is due to the tilt of the galactic plane, placing most of the molecular material below $b=0°$. Indeed, the small peak associated with the Carina nebula at $l=287°$ is quite literally only the top of the iceberg.

The maps show the CO distribution to be very clumpy; few cloud complexes extend over more than two degrees. This may in part be the effect, as mentioned in the preceding section, of our possible underestimation of broad-velocity, diffuse CO emission, resulting in a contrast enhancement of narrower-velocity components. As we will show below, it appears that the extended emission is at most diluted by a factor of two, so that the clumpiness observed in our maps is quite real. We conclude that in a qualitative sense the overall distribution of CO in the fourth galactic quadrant is well-represented in Fig. 2. This is illustrated by the overall good agreement between the CO($J=2-1$) map shown here, and the CO($J=1-0$) map obtained by the Australian group (Robinson et al., 1983). In particular, our map shows gaps in the CO(2–0) distribution at terminal velocities at longitudes $l=306°$–$309°$, $317°$–$320°$, $326°$–$329°$, $333°$–$336°$, and $337°$–$340°$, coincident with the holes in the CO(1–0) terminal distribution. In the same way the CO associated with the 4 kpc expanding arm shows up quite clearly. This good agreement also indicates that, for the majority of molecular clouds, the two lowest CO transitions behave very similarly, so that at least on scales of order two degree differences in optical depth do not play a significant role; a more detailed comparison is made by Brand et al., 1984).

3.2. Longitude distribution of integrated CO

In Fig. 4 we show the distribution of CO($J=2-1$) integrated over the full velocity range as a function of galactic longitude. For comparison, we also show the longitude distribution of integrated neutral hydrogen (H I) from the survey by Kerr et al. (1983). Again the relatively low intensity of the integrated CO emission below $l=300°$ is largely due to the tilt of the galactic plane. Above $l=300°$

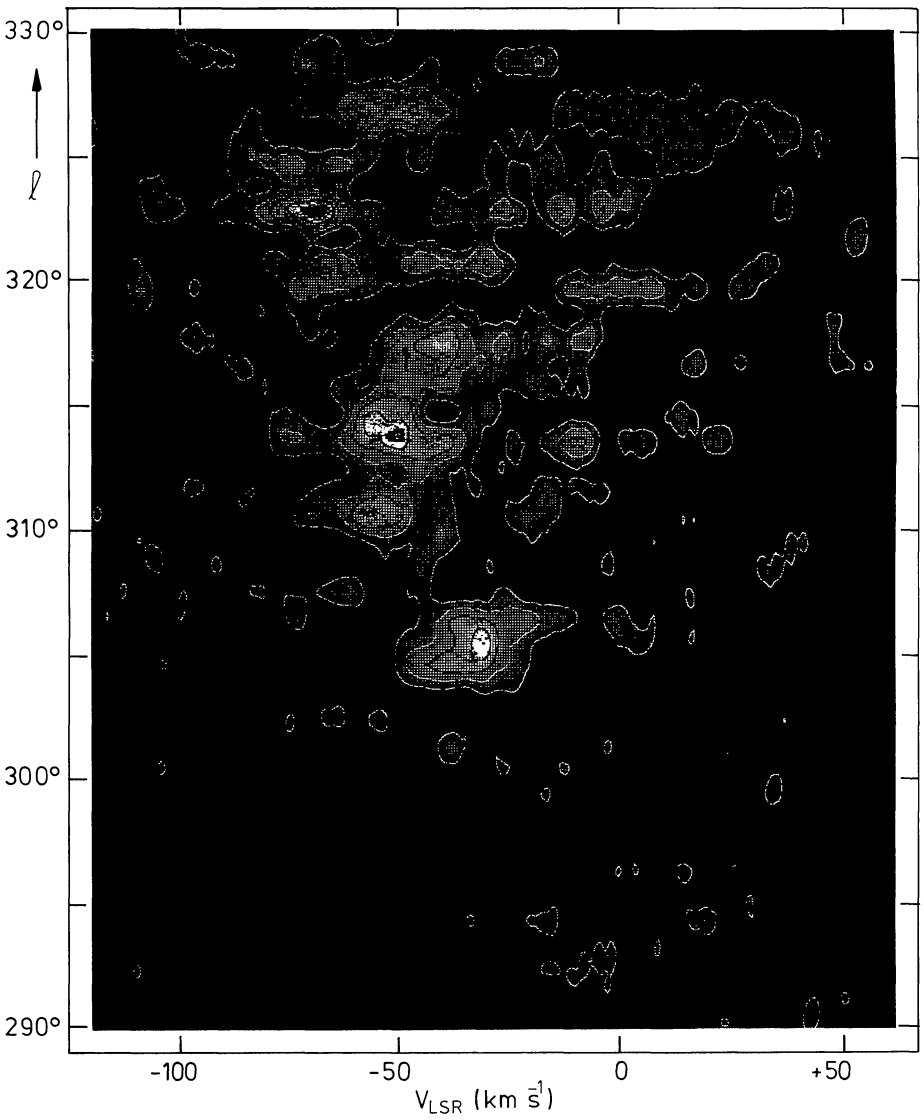

Fig. 3. Same as Fig. 2, but over a more limited range in longitude and averaged over one-degree intervals

Table 1. Brightest CO(2−1) maxima in the fourth quadrant

Longitude (°)	Size (°)	V_{LSR} (km s^{-1})	Vel. width (km s^{-1})	T_A^* (K)	Assoc. H II regions
287.0	1.5	− 27	10	1.7	RCW 53 Carina
305.5	3.1	− 38	25	2.2	RCW 74
311.5	2.6	− 59	15	2.3	G 311.5+0.3
315.0	2.5	− 58	40	3.5	
323.0	1.6	− 72	25	3.5	
327.0	1.9	− 50	20	2.3	RCW 97
334.0	2.1	− 92	30	2.2	RCW 106 Norma
	1.5	− 52	30	2.8	
336.5	1.7	−115	20	2.0	G 336.4−0.3
	1.7	− 79	15	2.0	
340.5	2.7	− 41	10	2.6	
342.8	2.7	− 32	20	2.5	G 343.5+0.0
	1.6	− 21	15	2.0	
344.4	2.3	−115	25	2.0	
	2.3	− 22	10	1.8	

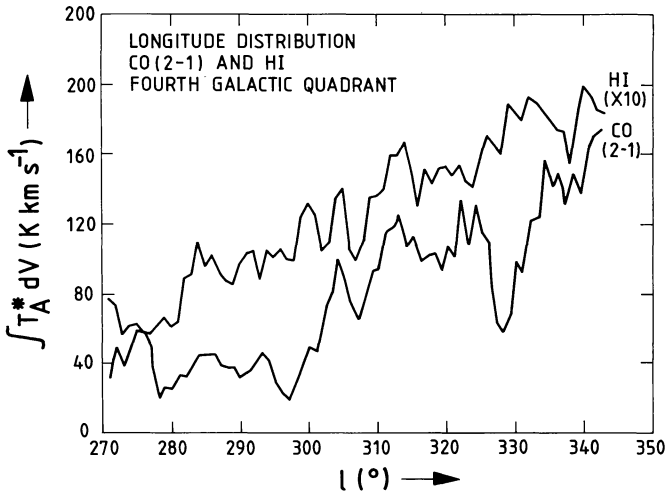

Fig. 4. Longitude distribution of CO ($J=2-1$) integrated over the velocity range -170 to $+60$ km s^{-1}. For comparison, also the H I distribution is shown

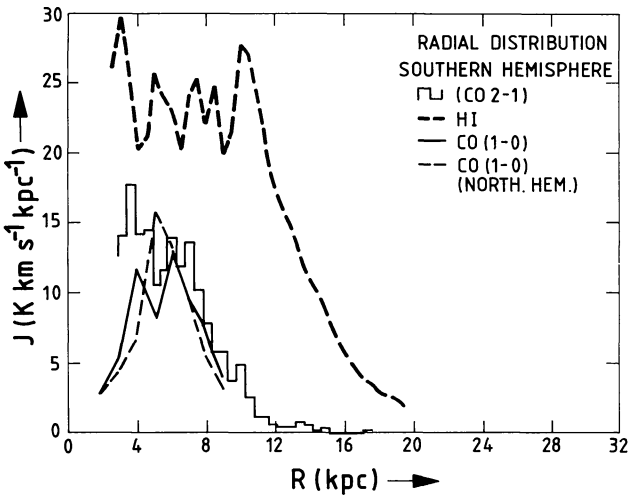

Fig. 5. Integrated CO ($J=2-1$) emissivities as a function of distance R to the Galactic Centre. The histogram indicates the southern hemisphere $2-1$ data, whereas solid lines indicate northern and southern hemisphere $1-0$ emissivities from Sanders (1981). The dashed line indicates the southern hemisphere H I emissivity derived from Kerr et al. (1983)

both CO transitions show the same rising trend but the rise of CO($2-1$) is not as rapid as that of CO($J=1-0$) (Robinson et al., 1983). This again may be the consequence of our dilution of broad-velocity emission, which in particular influences CO intensities integrated in velocity. Nevertheless, the overall CO($J=2-1$) and CO($J=1-0$) longitude distributions are very similar.

The lack of CO at the terminal velocities mentioned in the previous section also shows up in the integrated CO longitude distribution, but not so strikingly. Minima are seen near $l=298°$, 308°, 317°–320°, and 329°. The minimum at $l=308°$ is also found in the H I distribution. Most of the terminal lack of CO at these longitudes is, however, compensated by the relatively strong CO/H I maximum at $l=306°$ at less extreme velocities associated with the H II region complex RCW 74. The CO minima at $l=298°$ and $l=329°$ have no counterpart in integrated H I.

3.3. *Radial distribution*

If the rotation curve is known, the observed distribution of CO emission in velocity and longitude can be used to determine the radial distribution of CO in the galaxy. To this end, we have used the galactic rotation curve determined by Burton and Gordon (1978). Although this rotation curve was based on northern hemisphere data, Burton (private communication) has noted that southern hemisphere H I data (Kerr et al., 1983) are well represented by the same curve, shifted downwards (in an absolute sense) by 10 km s^{-1} in velocity. In Fig. 5 we show the resulting $J(R)$ CO($J=2-1$) emissivity (in K km s^{-1} kpc^{-1}) as a function of galactic radius R integrated over annuli of 0.5 kpc. Since the inner part of the Galaxy was poorly sampled, this procedure is meaningful only for radii $R>3$ kpc. The distribution of CO outside the solar circle is somewhat less certain; the distribution shown was obtained by taking into account a noise contribution to $J(R)$ of $T_A^*=0.5$ K. However, the level of the noise contribution used is not very critical. If we would not take into account a noise contribution, the CO emissivity at $R=12$ kpc would increase by a factor of two, but it would remain unchanged for $R<12$ kpc and $R>16$ kpc. In Fig. 5 we also show, for comparison purposes, the southern hemisphere H I radial emissivity (determined from the data by Kerr et al., 1983) and the northern and southern hemisphere CO($1-0$) radial emissivities (Sanders, 1981). As the figure shows, the CO($J=2-1$) emissivity has a broad maximum between $R=3.5$ kpc and $R=8$ kpc, and beyond that drops smoothly to zero at about $R=15$ kpc.

Comparison with the results obtained by Sanders (1981), Dame (1983) and Robinson et al. (1983) indicates that we may have missed at most 50% of the integrated CO emission at high longitudes (corresponding to low values of R) and probably less. They also show that the fine structure seen in the radial distribution maximum (i.e. peaks at $R=3.6$ and 7 kpc and a minimum at $R=5.5$ kpc) is probably real, since it corresponds to structure seen in the data obtained by Robinson et al. (1983) and Sanders (1981). This is in contrast to what is seen in H I: the H I emissivity is flat between $R=2.5$ and $R=11$ kpc, and only then drops to zero at $R=20$ kpc. The southern CO radial distribution also differs from the northern hemisphere distribution, where only a single, somewhat narrower and higher peak is seen. Thus, in both hemispheres the inner galaxy appears to contain appreciable amounts of molecular hydrogen (as traced by CO), but the structure of the "molecular ring" is different in the two galactic quadrants.

3.4. *Velocity dispersion*

In order to study the kinematics of the CO($J=2-1$) cloud ensemble we have plotted in Fig. 6 CO($2-1$) terminal velocities as a function of longitudinal, as well as H I terminal velocities. We have also included terminal velocities expected on the basis of the Burton and Gordon (1978) southern hemisphere galactic rotation curve mentioned in the preceding section. In addition, we give the velocities expected on the southern hemisphere rotation curve determined by Sinha (1978), which differ mainly in the inner galaxy. As is clear from Fig. 6, there is good general agreement between the observed terminal velocities and the model curves. In

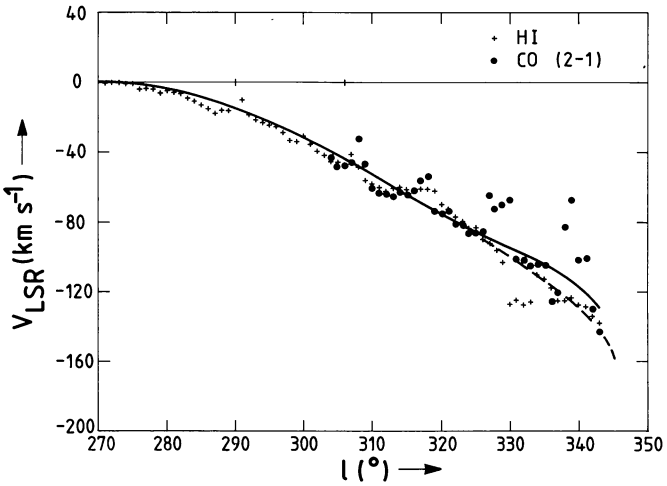

Fig. 6. CO($J=2-1$) terminal velocities (dots) as a function of Galactic longitude; H I terminal velocities are marked by crosses. The solid line indicates velocities expected on the basis of the revised Burton and Gordon (1978) rotation curve, the dashed line those expected on the basis of the Sinha (1978) rotation curve

the inner galaxy, the Sinha curve provides a slightly better fit than the Burton and Gordon curve.

Lack of CO – "CO holes" – is again seen at $l=307°$–$309°$, $315°$–$319°$, $326°$–$331°$, $338°$–$341°$, and perhaps around $l=335°$. Only the first two "CO holes" corresponds to an "H I hole". From the scatter of points outside these "holes" around the Burton and Gordon model curve, we derive an rms velocity dispersion of $4.5\pm0.5\,\mathrm{km\,s^{-1}}$ for the CO($J=2-1$) clouds at the tangential points; the rms dispersion for the Sinha curve is about $4.0\pm0.5\,\mathrm{km\,s^{-1}}$. At the same time, the rms velocity dispersion of CO tangential velocities with respect to H I tangential velocities is $3.7\pm0.5\,\mathrm{km\,s^{-1}}$. It should be noted that these values refer to an effective resolution of 1° to 2°; if clouds were to show significant velocity structure on smaller scales, the velocity dispersion could be somewhat higher. Nevertheless, there is good agreement with the result obtained for the northern hemisphere ($4.5\,\mathrm{km\,s^{-1}}$, Dame, 1983; $4.2\,\mathrm{km\,s^{-1}}$, Liszt and Burton, 1983).

4. Conclusions

We conclude that in the fourth galactic quadrant the distribution of CO($J=2-1$) is in several respects very close to that of CO($J=1-0$). We confirm the presence of "holes" in the CO distribution and its clumpy nature. CO terminal velocities follow very closely the curve predicted by model rotation curves (Burton and Gordon, 1978; Sinha, 1978). The rms cloud velocity dispersion is practically identical to that in the northern first galactic quadrant, but there is a small difference between the northern and southern radial CO distributions. Thus, the CO distribution in the first and the fourth galactic quadrant are essentially similar, but there are a few differences seen on a more detailed scale. Further studies should concentrate on these, as they may provide a key to our understanding of the detailed structure of our Galaxy, in particular that of the "molecular ring".

Acknowledgements. We are indebted to Dr. W. B. Burton for providing the computer program necessary to generate Figs. 5 and 6. We would also like to thank Dr. L. Woltjer for generously providing a substantial amount of observing time on the CAT during its commisioning phase, personnel at ESO – La Silla for technical help, Mr. F. Cornelis and Dr. H. Nieuwenhuyzen for considerable software support, and Drs. B. Fitton and D. E. Page for their encouragement and support in setting up and carrying out the southern survey work.

References

Brand, J.: 1982, *ESO Messenger* No. 29, p. 20
Brand, J., van der Bij, M.D.P., de Vries, C.P., Israel, F.P., de Graauw, Th., van de Stadt, H., Wouterloot, J.G.A., Leene, A., Habing, H.J.: 1984, *Astron. Astrophys.* (submitted)
Burton, W.B., Gordon, M.A.: 1978, *Astron. Astrophys.* **63**, 7
Cohen, R.S.: 1983, in *Surveys of the Southern Milky Way*, eds. W. B. Burton, F. P. Israel, Reidel, Dordrecht, p. 265
Dame, T.: 1983, Ph.D. Thesis, Columbia University
de Vries, C.P., Brand, J., Israel, F.P., de Graauw, Th., Wouterloot, J.G.A., van de Stadt, H., Habing, H.J.: 1984, *Astron. Astrophys. Suppl.* (in press)
Gustincic, J.J.: 1976, *Second Intern. Conf. on Submillimeter Waves and their Application*, San Juan, Puerto Rico
Kerr, F.J., Bowers, P.F., Kerr, M.: 1983 (in preparation)
Kutner, M.L., Ulich, B.: 1981, *Astrophys. J.* **250**, 341
Lidholm, S., de Graauw, Th.: 1979, *Fourth Intern. Conf. on Infrared and Submillimeter Waves and their Applications*, San Juan, Puerto Rico
Liszt, H.S., Burton, W.B.: 1983, in *Kinematics, Dynamics and Structure of the Milky Way*, ed. W. L. H. Shuter, Reidel, Dordrecht, p. 135
Robinson, B.J., Manchester, R.N., Whiteoak, J.B.: 1983, in *Surveys of the Southern Milky Way*, eds. W. B. Burton, F. P. Israel, Reidel, Dordrecht, p. 1
Sanders, D.B.: 1981, *Thesis, State University of New York, Stony Brook*
Sherwood, W.A., Schultz, G.V., Greve, A.: 1983, *Infrared Phys.* **23**, 109
Sinha, R.P.: 1978, *Astron. Astrophys.* **69**, 227